Journal of the Geological Society, London, Vol. **171**, 2014, pp. 709–722. http://dx.doi.org/10.1144/jgs2014-016
Published *Online First* on July 7, 2014

Revised Wonoka isotopic anomaly in South Australia and Late Ediacaran mass extinction

GREGORY J. RETALLACK[1*], ANDRÉ MARCONATO[2], JEFFERY T. OSTERHOUT[1], KATHRYN E. WATTS[3] & ILYA N. BINDEMAN[1]

[1]*Department of Geological Sciences, University of Oregon, Eugene, OR 97403-1272, USA*
[2]*Institute of Geosciences, University of São Paulo, Rua do Lago, 562, São Paulo, SP 05508-080, Brazil*
[3]*US Geological Survey, 345 Middlefield Road, Menlo Park, CA 94025, USA*
**Corresponding author (e-mail: gregr@uoregon.edu)*

Abstract: The global Late Ediacaran Shuram–Wonoka carbon isotope anomaly has been regarded as the largest and longest known isotopic anomaly in the ocean, assuming that all Ediacaran carbonate is marine. Disregarding carbonate in South Australia shown here to be palaeosol or palaeokarst, the synchronous marine organic–carbonate excursion is only −8‰ for $\delta^{13}C$ organic and −6‰ for $\delta^{13}C$ carbonate, and lasted less than a million years. This revised magnitude and duration is comparable with perturbations across the Permian–Triassic boundary, and correlative with a global Late Ediacaran acritarch mass extinction. Like Permian–Triassic isotopic excursions, the revised organic–carbonate Wonoka excursion may also have been a greenhouse palaeoclimatic warm spike, which terminated valley incision and glacioeustatic drawdown during the mid-Ediacaran Fauquier Glaciation, and preceded chill of the Late Ediacaran Billy Springs Glaciation.

Supplementary material: Measured sections and tables of mineral and grain-size proportions, major element and stable isotope analyses are available at www.geolsoc.org.uk/SUP18756.

The Ediacaran Period some 541–635 Ma ago (Gradstein *et al.* 2012) is characterized by large multicellular organisms (Vendobionta: Jenkins & Nedin 2007; Retallack 2013*a*) and a distinctive assemblage of large ornamented acritarchs (Grey 2005; Gaucher & Sprechmann 2009). The Ediacaran also includes the earliest known mass extinction: diverse Ediacaran acritarchs (ECAP or Ediacaran Complex Acanthomorph-dominated Palynoflora assemblage of Grey 2005) are replaced with a low-diversity 'Kotlin–Rovno' or LELP (Late Ediacaran Leiosphere-dominated Palynoflora) of Gaucher & Sprechmann (2009). These biological events may have coincided with fluctuations in oxygenation of the atmosphere (Fike *et al.* 2006; McFadden *et al.* 2008). Critical to understanding these fluctuations has been a carbonate carbon isotope excursion considered the longest and deepest in Earth history (Grotzinger *et al.* 2011), which has been correlated between Oman (Shuram anomaly of Burns & Matter 1993), South Australia (Wonoka anomaly of Calver 2000), South China (DOUNCE anomaly of McFadden *et al.* 2008; Lu *et al.* 2013) and southwestern USA (anomaly of Rainstorm Member of Corsetti & Kaufman 2003). The basis for such global chemostratigraphic correlation is the assumption that the isotopic anomaly records a dramatic change in the isotopic composition of dissolved inorganic carbon in seawater (Halverson *et al.* 2005). Shuram–Wonoka isotopic depletion is so extreme (down to −15.7‰ from −1.4‰ in $\delta^{18}O$ of carbonate, and down to −11.33‰ from +0.95‰ in $\delta^{13}C$ of carbonate: Calver 2000) that the most negative parts of the anomaly require unusual marine methane emissions (Bjerrum & Canfield 2011), or overturn of an isotopically stratified ocean (Calver 2000; Swanson-Hysell *et al.* 2010). Neither marine mechanism explains observed correlation between $\delta^{13}C_{carb}$ and $\delta^{18}O_{carb}$ in many (but not all) excursions worldwide (Grotzinger *et al.* 2011), so that alternative explanations of diagenetic alteration of marine limestones have been proposed. In one diagenetic scenario the marine limestones are considered altered by light carbon from soil respiration within meteoric water, which can flush many hundreds of metres down around tropical islands today (Knauth & Kennedy 2009; Swart & Kennedy 2012). A second diagenetic scenario is mixing of two distinct deep formation waters: a low-$\delta^{13}C$ fluid from cracking of buried organic matter and a low-$\delta^{18}O$ basinal brine (Derry 2010).

This paper proposes and tests a fifth, and new, mechanism for the development of the Wonoka isotopic anomaly in South Australia, by Ediacaran soil formation, including both development of pedogenic carbonate (caliche) and surficial weathering ('meteoric diagenesis') of pre-existing marine carbonate (palaeokarst). Palaeosols and palaeokarsts have been recognized in Ediacaran rocks from micritization, ferruginization, cracking and sand crystals (Kaufman *et al.* 2006; Retallack 2011, 2012, 2013*a*; Xiao *et al.* 2013). Palaeosols show open-system use of CO_2, which bestows a highly significant correlation between $\delta^{13}C_{carb}$ and $\delta^{18}O_{carb}$ values (Ufnar *et al.* 2008). Previous chemostratigraphic studies of Ediacaran carbonate have assumed that it was all marine, with few samples rejected for diagenetic or hydrothermal alteration (Calver 2000; Grotzinger *et al.* 2011), but this study assessed the field setting of each analysed carbonate as well as petrographic and geochemical indications of potential palaeosols. The Wonoka carbon isotopic anomaly is at the same stratigraphic level as remarkable erosional features controversially interpreted as subaerial (Eickhoff *et al.* 1988; von der Borch *et al.* 1989; Christie-Blick *et al.* 1990) or submarine canyons (von der Borch *et al.* 1985; Giddings *et al.* 2010). This documentation of palaeosols of the Bunyeroo and Wonoka Formations and of the Bonney Sandstone evaluates hypotheses for both the Shuram–Wonoka carbon isotope anomaly and for associated palaeocanyons in South Australia, and their relevance for Ediacaran life and palaeoclimate.

Materials and methods

Fieldwork involved sampling of Ediacaran palaeosols in South Australia (Fig. 1; Retallack 2011, 2012, 2013*a*), with emphasis on a master section (Figs 2 and 3), combining Brachina Gorge (Mawson 1939*a*) and Ten Mile Creek sections (Mawson 1939*b*). Fieldwork

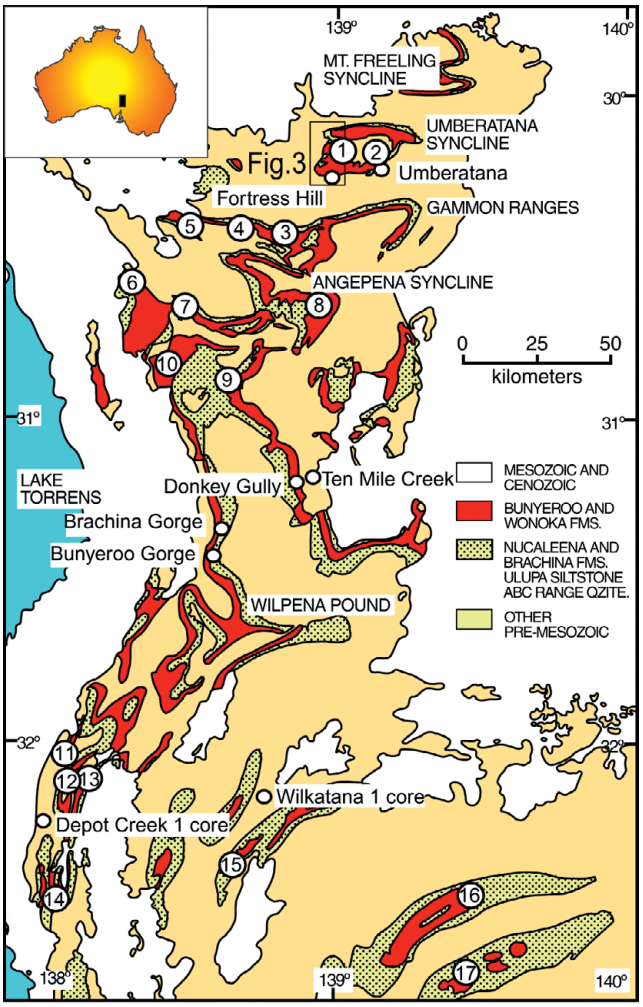

Fig. 1. Study localities on a simplified geological map of the Bunyeroo and Wonoka Formations in the Flinders Ranges, South Australia. Numbered circles are palaeocanyons within the Wonoka Formation: 1, Fortress Hill; 2, Umberatana; 3, Oodnapanicken; 4, Depot Springs; 5, Patsy Springs; 6, Nankabunyana; 7, Salt Creek; 8, Mocatoona; 9, Puttapa; 10, Beltana; 11, Buckaringa Hill; 12, Buckaringa Gorge; 13, Yarra Vale; 14, Waukarie Creek; 15, Pamatta Pass; 16, Waroonee; 17, Yunta.

also made site assessments for carbonate analysed in previous studies (Eickhoff *et al.* 1988; Calver 2000; McKirdy *et al.* 2001; Swanson-Hysell *et al.* 2010). In Brachina Gorge, sections of Bonney Sandstone were measured in the long exposure beneath the Chace Quartzite Member of Rawnsley Quartzite (Figs 4a and 5; 31.34374°S, 138.56279°E), and of Patsy Hill Member 0.5 km west in the gorge (31.34193°S, 138.56886°E), where it was similar to exposures on the ridge 0.6 km to the north (31.33613°S, 138.56824°E). Observations at each isotopic sampling locality of Calver (2000) and at the *Palaeopascichnus* locality of Haines (2000) were also made in a transect of Bunyeroo Gorge, from the Acraman impact bed of the Bunyeroo Formation (Fig. 6; Gostin *et al.* 2010) in the creek near the western car-park (31.41576°S, 138.55870°E) west to the Ediacara Member of the Rawnsley Quartzite (41.41401°S, 138.54212°E). Acraman ejecta in the Bunyeroo Formation were also examined in Donkey Gully, in the headwaters of Balcoracana Creek (32.22362°S, 138.84974°E). Palaeocanyons (Fig. 3) of Eickhoff *et al.* (1988) and von der Borch *et al.* (1989) were sampled NW of Umberatana Station (30.232901°S, 139127363°E) and north of Fortress Hill (30.19275°S, 138.9919°E). Also examined were red beds in core at the Primary Industries South Australia (PIRSA) core depository in the Adelaide suburb of Glenside (Fig. 4c): Wonoka Formation in Depot Creek core from 33 km north of Port Augusta (32.2310199°S, 137.9413394°E; Preiss & Faulkner 1984) included a Vulda palaeosol at 436.9 m and an Arru palaeosol at 439 m (Table 1), and Bunyeroo Formation in Wilkatana 1 core from 32 km east of Cradock (32.1247288°S, 138.830111°E; Preiss & Faulkner 1984) included many Vulda palaeosols at 435.5–523.6 m and an Arru palaeosol at 523.6 m.

Samples were collected to characterize mineral composition, grain size, major element and stable isotopic composition of single beds considered potential palaeosols within short measured sections. Petrographic thin sections were point counted (500 points) for grain size and mineral content, using a Swift® automatic point counter and stage. Selected samples were analysed for major elements using XRF, and for ferrous iron using Pratt titration, by ALS Chemex of Vancouver, BC, against standard SY-4 (diorite gneiss from Bancroft, Ontario). Analyses of $\delta^{13}C$ and $\delta^{18}O$ of carbonate were made using a Finnegan MAT 253 mass spectrometer in the Department of Geological Sciences, University of Oregon, against Vienna PDB standard.

Hydrolytic chemical reactions characteristic of soil formation were investigated by calculating molar ratios designed to reveal particular soil-forming processes. In addition, bulk density of all samples was calculated using paraffin-coated clods in water (Retallack 1997) to calculate gains and losses (mass transfer of Brimhall *et al.* 1992) of elements in a soil at a given horizon ($\tau_{w,j}$ in moles) from the bulk density of the soil (ρ_w in g cm^{-3}) and parent material (ρ_p in g cm^{-3}) and from the chemical concentration of the element in soils ($C_{j,w}$ in wt%) and parent material ($C_{j,p}$ in wt%). Subscripts are for soil (w), parent material (p), mobile element (j) and immobile element (j). Also needed are changes in volume of soil during weathering (strain of Brimhall *et al.* 1992), estimated from an immobile element in soil (such as Ti used here) compared with parent material ($\varepsilon_{i,w}$ as a fraction). The following equations are the basis for calculating divergence from parent material composition:

$$\tau_{j,w} = \left[\frac{\rho_w \cdot C_{j,w}}{\rho_p \cdot C_{j,p}}\right]\left[\varepsilon_{i,w} + 1\right] - 1 \quad (1)$$

$$\varepsilon_{i,w} = \left[\frac{\rho_p \cdot C_{j,p}}{\rho_w \cdot C_{j,w}}\right] - 1. \quad (2)$$

Geological background

The Ediacaran Period in the Flinders Ranges of South Australia is represented by the Wilpena Group, consisting of the Nuccaleena Formation to Rawnsley Quartzite (Fig. 1). This thick sequence of

Fig. 2. Long record of palaeosols, palaeokarst and marine carbonate stable isotopic variation in the Flinders Ranges, South Australia, showing different concepts of the Wonoka carbon isotopic excursion of Calver (2000) and as revised here: (**a**) composite stratigraphic section in Brachina Gorge (Mawson 1939*a*) and Ten Mile Creek (Mawson 1939*b*): (**b**) depth to calcareous nodules in moderately developed palaeosols (Retallack 2008, 2011, 2012): (**c**–**e**) stable isotope compositions of organic matter, of palaeosol carbonate (caliche nodules), palaeokarst (micritized and ferruginized limestone) and unaltered marine carbonate (data from Eickhoff *et al.* 1988; Calver 2000; McKirdy *et al.* 2001; Retallack 2008, 2012; Swanson-Hysell *et al.* 2010; and herein), with named isotopic excursions (after Halverson *et al.* 2005; Gradstein *et al.* 2012) and glaciations (Williams *et al.* 2008; Hebert *et al.* 2010; Landing & McGabhann 2010; Jenkins 2011). Compaction-corrected mean annual precipitation is derived from depth to Bk by algorithms of Sheldon & Retallack (2001) and Retallack (2005).

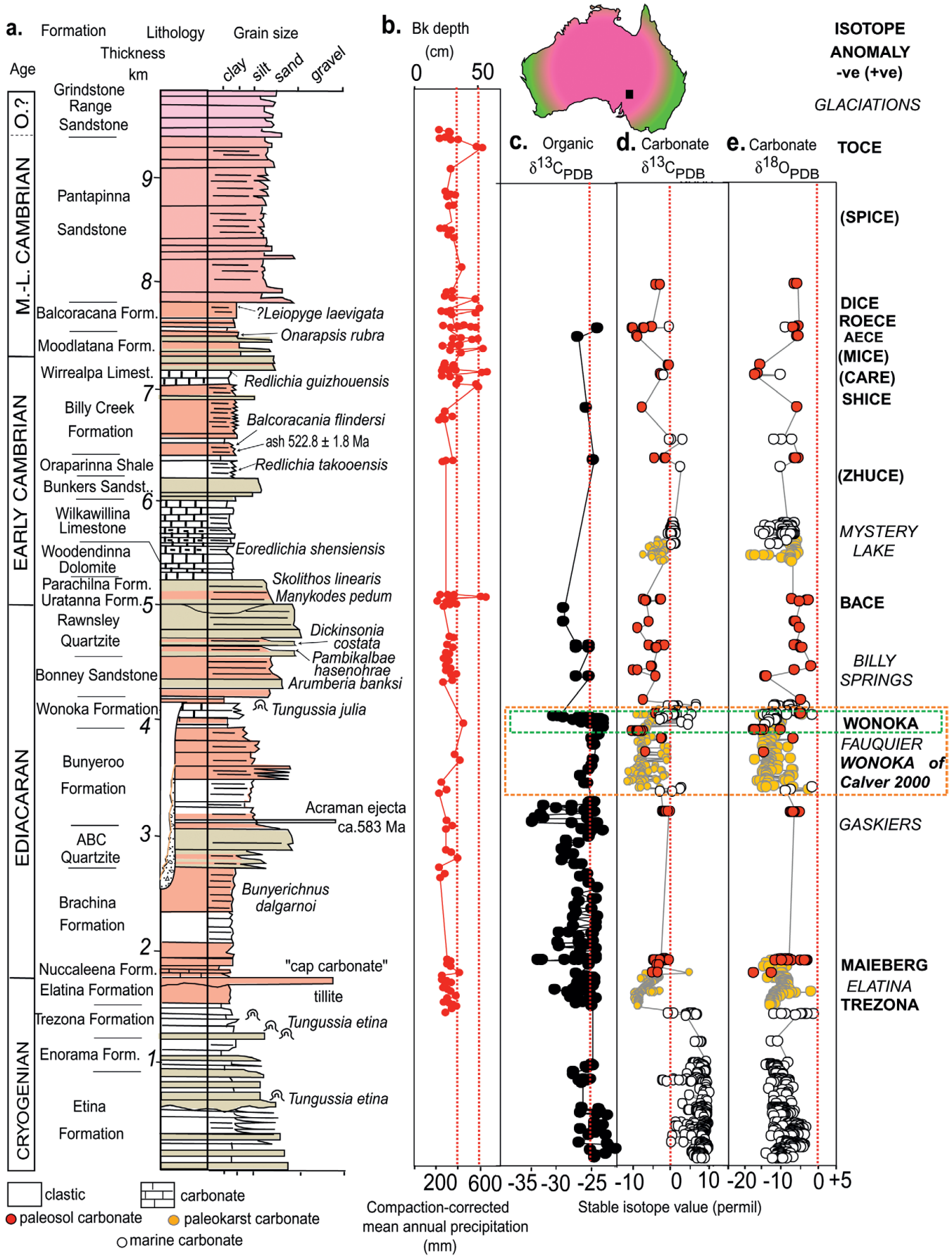

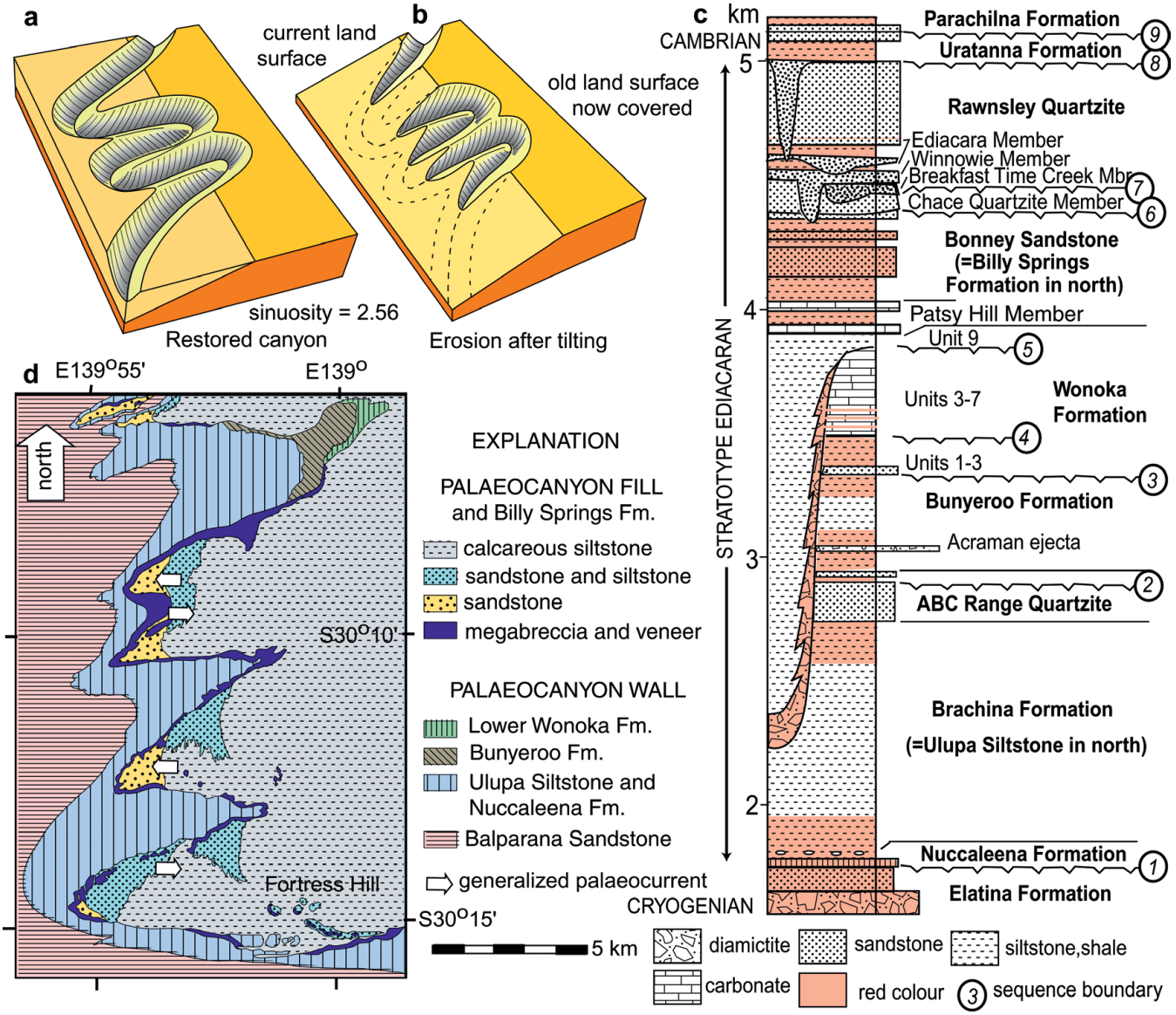

Fig. 3. Reconstruction (**a**, **b**) and geological map (**d**) of Fortress Hill meandering palaeocanyon, and its stratigraphic position at sequence boundary 5 in the Wonoka Formation (**c**). (**a**) and (**b**) are modified from von der Borch *et al.* (1989), and (**c**) is from Mawson (1939*a*), Christie-Blick *et al.* (1990), Jenkins & Nedin (2007) and Husson *et al.* (2012).

quartzofeldspathic sandstone and siltstone, with interbedded limestone and dolostone (Fig. 2), accumulated on a passive continental margin (Drexel *et al.* 1993). Local deformation was created by synsedimentary intrusion of diapiric breccias, perhaps related to salt mobilization (Dyson 2003; Backé *et al.* 2010; Kernen *et al.* 2012). The Wonoka Formation is mainly carbonate–nodular shale and calcarenitic limestone, and according to Calver (2000) the Wonoka–Shuram isotopic anomaly is found through most of the formation (beds 3–8 inclusive, 75–654 m above the base of the formation). Red beds formerly of upper Wonoka Formation (beds 9–11 of Haines 1988) are above the isotopic anomaly and are now assigned to the Patsy Hill Member of the Bonney Sandstone (Reid & Preiss 1999).

The Wonoka Formation also hosts spectacular palaeocanyons (Fig. 3), which Christie-Blick *et al.* (1990) correlated with sequence boundaries above Wonoka Formation units 1 and 3 of Haines (1988). An 'isotopic conglomerate test', matching carbon isotopic composition in walls and fill, by Husson *et al.* (2012) concluded that the erosional surface from which palaeocanyons developed was at least above unit 7 of the Wonoka Formation, and perhaps higher. This matches observed abundance of large limestone clasts in the palaeocanyon fill (Fig. 4f). One palaeocanyon 1500 m deep was the Fortress Hill–Umberatana complex (von der Borch *et al.* 1985), but the nearby Patsy Springs palaeocanyon was 900 m deep (von der Borch *et al.* 1989), and the Oodnapanicken and Mount Goddard palaeocanyons were 700 m deep (Husson *et al.* 2012).

Ediacaran age of the Wonoka Formation is established by megafossils (*Palaeopascichnus*; Haines 2000), complex acritarchs (ECAP: Grey 2005), and stromatolites (*Tungussia*; Walter *et al.* 1979). Also Ediacaran are megafossil fronds or straps (*Bunyerichnus dalgarnoi*) in the Bunyeroo Formation (Fedonkin *et al.* 2008), and discoids, small fronds, *Arumberia* and tiny 'cocoons' like testate amoebae (Porter *et al.* 2003) in the overlying Bonney Sandstone (Haines 1987; Jenkins & Nedin 2007). These are all statigraphically below the classical Ediacaran biota of the Ediacara Member of the Rawnsley Quarzite (Fedonkin *et al.* 2008; Retallack 2013*a*).

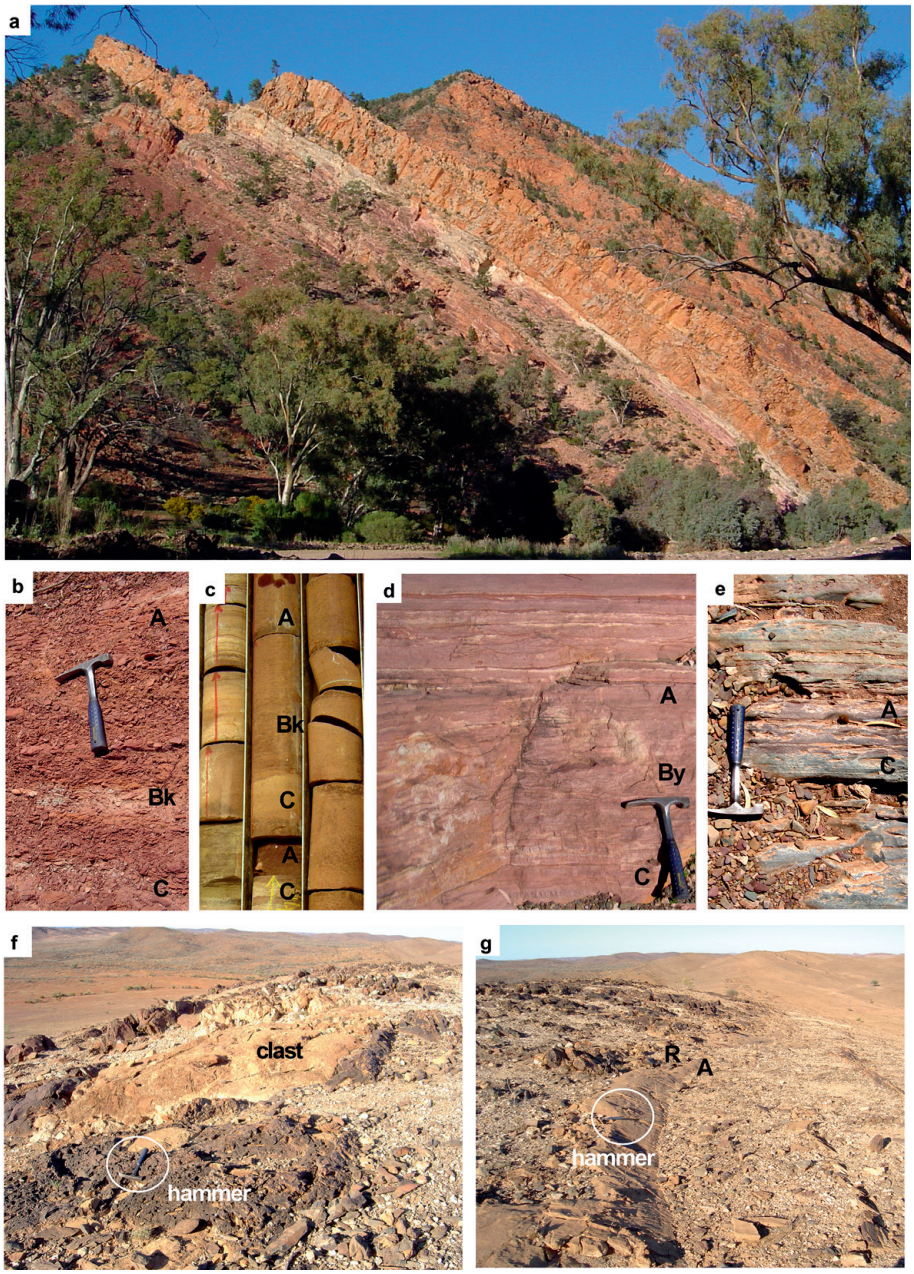

Fig. 4. Field and core photographs: (**a**) fluvial facies of Bonney Sandstone and overlying Chace Quartzite of the Rawnsley Quartzite in central Brachina Gorge; (**b**) type Yaldati silty clay loam palaeosol from Ediacara Member of Rawnsley Quartzite in Brachina Gorge; (**c**) Vulda (above centre) and Arru (below centre) palaeosols, flanked by Vulda palaeosol (right) and red–green intertidal facies (left) at 450 m in Bunyeroo Formation of Wilkatana 1 core; (**d**) Muru sandy loam palaeosol of Bonney Sandstone in Brachina Gorge; (**e**) type Arku loam palaeosol of Wonoka Formation in Bunyeroo Gorge; (**f**) palaeocanyon-fill megabreccia in Wonoka Formation NW of Umberatana Station; (**g**) Vidla silt loam palaeosol ('veneer' of Eickhoff *et al.* 1988) atop palaeocanyon megabreccia NW of Umberatana Station. Hammer for scale (**b**, **d**–**g**) is 25 cm long, and core (**c**) has diameter 5 cm.

Radiometric dating in the Ediacaran of South Australia is sparse, but four points can be used to construct an age model for the Brachina Gorge section measured by Mawson (1939*a*): (1) 541 ± 0.63 Ma for Cambrian–Ediacaran boundary at 5009 m at top of Rawnsley Quartzite (Gradstein *et al.* 2012); (2) 558 ± 48 Ma for detrital zircon from 4326 m in Bonney Sandstone (Ireland *et al.* 1998); (3) 582.4 ± 0.5 Ma for dropstones at 3223 m in the Bunyeroo Formation correlated by Gostin *et al.* (2010) with the Gaskiers Glaciation of Newfoundland (van Kranendonk *et al.* 2008) and also the Croles Hill Diamictite of Tasmania (Calver *et al.* 2013); (4) Ediacaran–Cryogenian boundary best dated at 635.0 Ma (Gradstein *et al.* 2012). A linear model for age (A) from stratigraphic level (M)

$$A = -0.0297M + 686.49 \quad (3)$$

has reasonable accuracy ($R^2 = 0.98$, SE ±6 Ma).

From this age model, the predicted ages of various levels (of Haines 1988) in the Wonoka Formation are as follows: 581 ± 6 Ma for the base of unit 3 and onset of the Shuram–Wonoka excursion of Calver (2000) at 3536 m, 567 ± 6 Ma for top of unit 7 and palaeoplateau incised by palaeocanyons at 4037 m, and 564 ± 6 Ma for base of unit 10 and end of Shuram–Wonoka Formation at 4116 m. The Shuram–Wonoka excursion of Calver (2000) thus extended through at least 580 m, not counting up to 1500 m in some palaeocanyons (von der Borch *et al.* 1985), and so lasted for some 17 Ma (in the age model of equation (3)). During this long time the negative isotopic excursion was −8‰ for $\delta^{13}C$ organic and −12‰ for $\delta^{13}C$ carbonate, making it the most profound isotopic excursion ever (Grotzinger *et al.* 2011).

This paper takes a narrower view of only that part of the Wonoka excursion defined by both organic and carbonate carbon isotopic values in marine samples (Fig. 2), and this revised excursion

Table 1. *Pedotypes of the Bonney, Wonoka and Bunyeroo Formations*

Pedotype	Diagnosis	Soil Survey Staff (2010)	Food and Agriculture Organization (1975, 1978)	Australian (Isbell 1996)
Vulda	Red–green mottled siltstone (A horizon) and some relict bedding, above small calcareous mottles (Bk horizon)	Calciustept	Calcic Cambisol	Hypocalcic Calcarosol
Arku	Red ferruginized and micritized limestone (A) over bedded limestone (R)	Orthent	Lithosol	Leptic Rudosol
Arru	Red–green mottled siltstone (A horizon) with some relict bedding above clearly bedded grey siltstone (C horizon)	Fluvent	Calcaric Fluvisol	Stratic Rudosol
Inga	Grey sandstone capped with algal wrinkling and expansion cracks, with shallow and sparse red mottles (A horizon), over deeper sand-crystal rosettes (By horizon)	Haplogypsid	Gleyic Solonchak	Gypsic Calcarosol
Muru	Red massive siltstone to sandstone surface (A horizon), over a shallow horizon of hard, ellipsoidal, non-calcareous nodules with enclosed crystal pseudomorphs (By horizon)	Haplogypsid	Gypsic Yermosol	Gypsic Calcarosol
Vidla	Reddish yellow micritized limestone (A horizon) over bedded grey limestone and breccia (C horizon)	Orthent	Lithosol	Leptic Rudosol
Wadni	Red siltstone with ferruginized and cracked surface (A) over bedded red siltstone (C)	Fluvent	Eutric Fluvisol	Stratic Rudosol
Yaldati	Red siltstone with intensely reddened and expansion-cracked surface (A horizon) and some relict bedding, above ellipsoidal calcareous mottles (Bk horizon)	Haplocalcid	Calcic Xerosol	Calcic Calcarosol

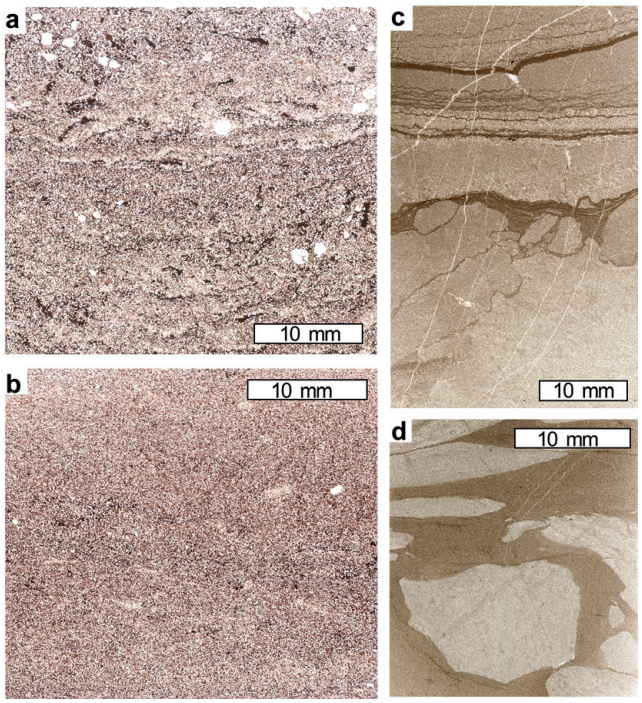

Fig. 5. Petrographic thin sections cut vertical to bedding of (**a**, **b**) Vulda sandy clay loam palaeosol (A and Bk horizon respectively) of the upper Wonoka Formation in Brachina Gorge, and (**c**, **d**) Vidla silt loam (A and C horizon respectively) of Wonoka Formation NW of Umberatana Station. Thin sections in Condon Collection of Museum of Natural and Cultural History, University of Oregon, are (**a**) R3476, (**b**) R3477, (**c**) R3656 and (**d**) R3654.

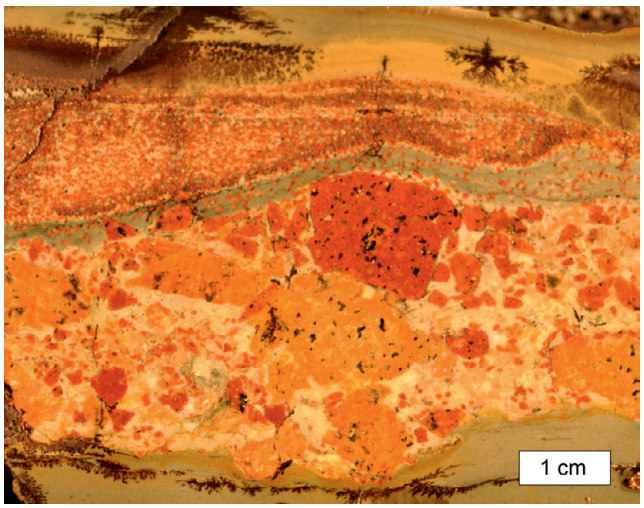

Fig. 6. Polished slab of ejecta of the Acraman impact above the Vulda silty clay loam drab surface variant palaeosol of the lower Bunyeroo Formation in Bunyeroo Gorge. Lack of grading by grain size is evidence that these ballistically emplaced fragments of dacite and red palaeosol from the impact crater could not have fallen though water, but were deposited on land.

was completed within 30 m, which corresponds to only 0.9 Ma at 564 ± 6 Ma. Furthermore, excluding analyses of carbonate from oxidized and other indications of palaeokarst or palaeosol limestone, the isotopic excursion was only −8‰ for $\delta^{13}C$ organic and −6‰ for $\delta^{13}C$ carbonate. Glacial dropstones and deformed beds of the Billy Springs Formation near Fortress Hill are 50 m above the Wonoka Formation (Jenkins 2011), and thus 563 ± 6 Ma by the age model of equation (3). Wonoka palaeocanyon incision at 567 ± 6 Ma by the age model is of comparable age with the Shuram–Wonoka excursion, *Tungussia julia* stromatolites, and glacial pavements and diamictites of the Egan and Boonall Limestones of northwestern Australia (Corkeron 2007). In Virginia, USA, a glacial diamictite (Rockfish Conglomerate Member) and a 'cap carbonate' of the Fauquier Formation of comparable ages are immediately below Catoctin Volcanics dated at 571 ± 1 Ma by zircon U–Pb (Hebert *et al.* 2010).

Although the Cryogenian Period is named for global glaciations (Halverson *et al.* 2005; Williams *et al.* 2008), there were several Ediacaran and Cambrian glacial advances potentially useful for international correlation, in addition to the Gaskiers Glaciation (Retallack 2013*b*), now dated at 583.7 ± 0.5 to 582.4 ± 0.5 Ma (van Kranendonk *et al.* 2008). An early Cambrian (*c.* 531 Ma or Terreneuvian) glacial advance is represented by dropstones and diamictites in the Mystery Lake Member of the upper Chapel Island Formation, near St. Johns, New Brunswick, Canada, and dropstones in the Booley Bay Formation of Ireland (Landing & McGabhann 2010).

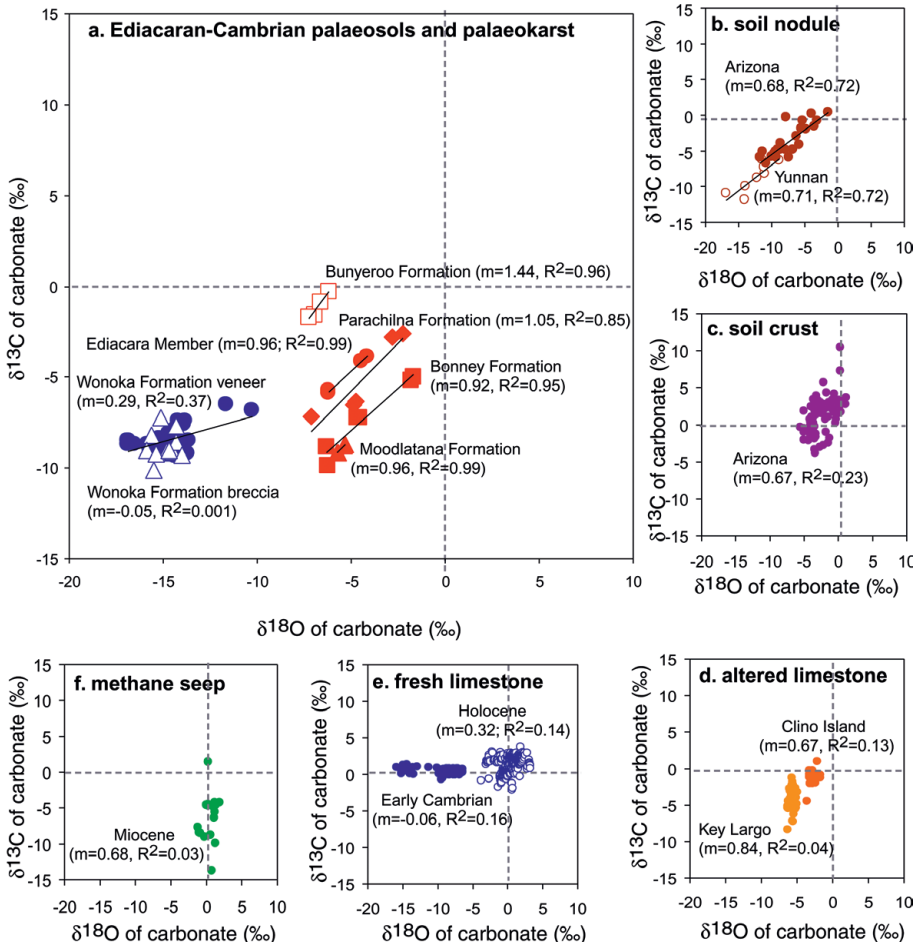

Fig. 7. Distinct arrays of carbon and oxygen isotopic composition of carbonate in (**a**) Ediacaran palaeosols of South Australia (Eickhoff *et al.* 1988; Retallack 2008, 2012; Giddings *et al.* 2010; herein) compared with known patterns of (**b**) soil nodules (above Woodhouse lava flow, near Flagstaff, Arizona, from Knauth *et al.* 2003; and in Yuanmou Basin, Yunnan, China, from Huang *et al.* 2005), (**c**) soil crusts on basalt (Sentinel Volcanic Field, Arizona, from Knauth *et al.* 2003), (**d**) Quaternary marine limestone altered diagenetically by meteoric water (Key Largo, Florida, from Lohmann 1988, and Clino Island, Bahamas, from Melim *et al.* 2004) (**e**) unweathered marine limestone (Holocene, from Veizer et al. 2000, and Early Cambrian, Ajax Limestone, South Australia, from Surge *et al.* 1997), and (**f**) marine methane cold seep carbonate (Miocene, Santa Cruz Formation, Santa Cruz, California, from Aiello *et al.* 2001). Slope of linear regression (*m*) and coefficients of detemination (R^2) show than carbon and oxygen isotopic composition is significantly correlated in soils and palaeosols.

Non-marine carbonate isotopic compositions

Palaeosols

The diagnostic isotopic signature of palaeosol carbonate is highly significant correlation of $\delta^{13}C$ and $\delta^{18}O$ and very light values for each isotope. Only soils show unusually negative values for both isotopes and highly correlative relationships (Fig. 7b) comparable with those observed in Cambrian and Ediacaran formations of South Australia (Fig. 7a). These correlations are created by evaporative selection for CO_2 in soils (Ufnar *et al.* 2008), and gain added significance from the large range of isotopic composition found in pedogenic rather than marine carbonates (Retallack *et al.* 2004). Tight correlations are observed only for palaeosols of small areas and particular geological formations, because the isotopic composition of soil CO_2 varies with vegetation and climate (Ufnar *et al.* 2008). For this reason, only isotopic compositions of soil nodules above Woodhouse lava flow, near Flagstaff, Arizona, are shown for comparison (Fig. 7b), rather than those of other flows or areas in Arizona, which combined show less significant correlations (Knauth *et al.* 2003). A better match for absolute isotopic values of Ediacaran palaeosols is the isotopic composition of soil nodules in the high elevation and inland Yuanmou Basin of Yunnan Province, China (Fig. 7b; Huang *et al.* 2005). Moderately significant correlations and surprisingly positive values for both $\delta^{13}C$ and $\delta^{18}O$ are found on carbonate crusts on basalt, such as those shown here from the Sentinel Volcanic Field, of Arizona (Fig. 7c), and attributed to extreme evaporation of sun-heated water films (Knauth *et al.* 2003). Marine limestone altered by deep circulation of meteoric water also shows a vague positive correlation, as shown here (Fig. 7d) by Neogene marine limestones of Key Largo, Florida (Lohmann 1988), and a borehole on Clino Island, Bahamas (Melim *et al.* 2004). Unaltered marine limestone shows no hint of correlation and is clustered near zero for both $\delta^{13}C$ and $\delta^{18}O$, as demonstrated by 420 analyses of Holocene sea shells and corals (Fig. 7e: Veizer *et al.* 2000). Also shown in Figure 7e are analyses of Early Cambrian, Ajax Limestone (laterally equivalent to Wilkawillina Limestone of Fig. 2) of South Australia (Surge *et al.* 1997), known to be marine because of its trilobites and abundant archaeocyathids. The offset of Cambrian versus Holocene $\delta^{18}O$ compositions is part of a long-term secular trend in $\delta^{18}O$ composition of seawater, so that Ediacaran oceans were *c.* 10‰ lighter than modern ones, perhaps owing to changes in ocean crust hydrothermal regime (Kasting *et al.* 2006). Yet another pattern of near constant $\delta^{18}O$ but highly varied $\delta^{13}C$ is seen in carbonate of marine methane cold seeps, as in the late Miocene, Santa Cruz Formation of Santa Cruz, California (Fig. 7f; Aiello *et al.* 2001). Methanogenic carbonate $\delta^{13}C$ can also be extremely negative: down to −48‰ in marine methane seeps (Peckmann *et al.* 2002) and down to −43‰ in wetland palaeosols (Ludvigson *et al.* 2013). This pattern resembles the 'meteoric sphaerosiderite lines' of wetland palaeosols (Ludvigson *et al.* 1998), and arises because of the dominance of $\delta^{18}O$ composition by water in waterlogged to aquatic habitats. Like most of the patterns in Figure 7, this one is unlike that for Ediacaran pedogenic carbonates (Fig. 7a).

Other petrographic and geochemical observations confirm that many beds of the Bunyeroo and Wonoka Formation and Bonney Sandstone were palaeosols. These beds were sampled in detail

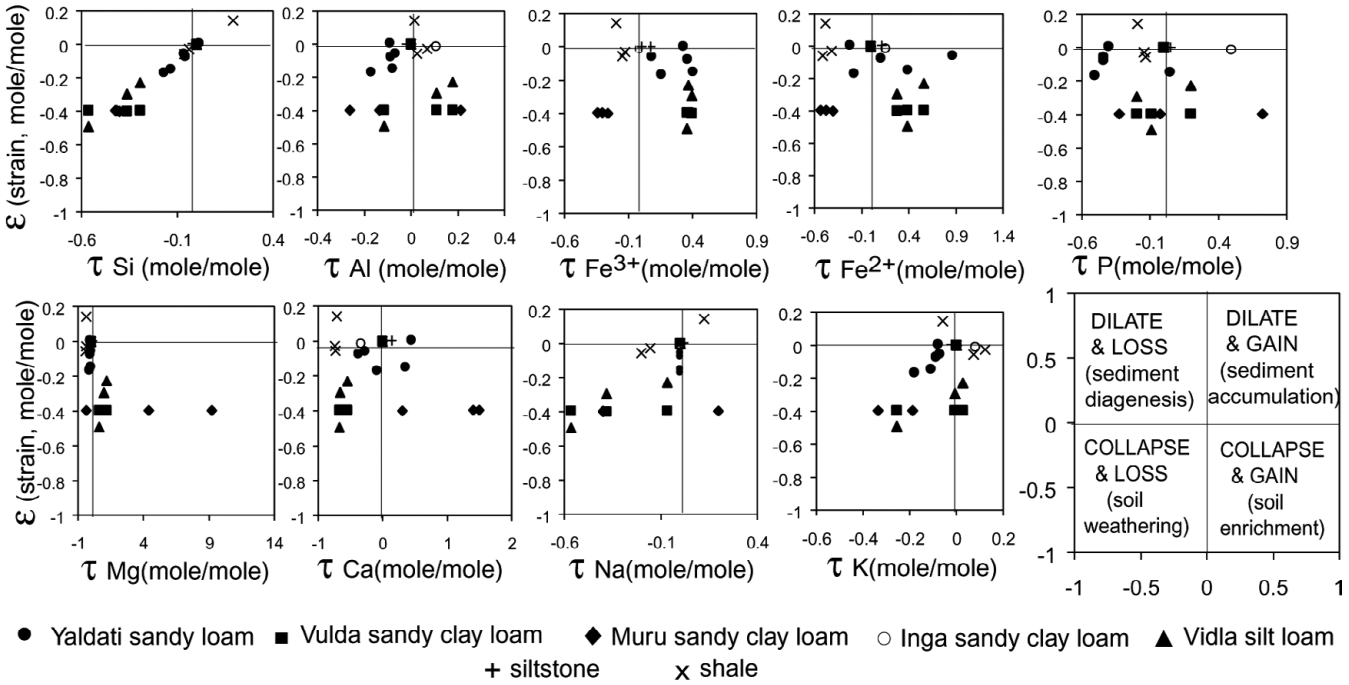

Fig. 8. Distinctive mass-balance geochemistry of Ediacaran palaeosols contrasted with sedimentary beds of South Australia, including estimates of strain from changes in an element assumed stable (Ti) and elemental mass transfer with respect to an element assumed stable (Ti, following Brimhall *et al.* 1992). Zero strain and mass transfer is the parent material lower in the profile: higher horizons deviate from that point owing to soil formation or sedimentation as indicated in key to lower right.

because they had an array of soil horizons (massive upper layers sharply overlain, diffuse horizons of calcareous or siliceous nodules) and soil structures (nodules, bedding disruption), as in other Cambrian and Ediacaran palaeosols of South Australia (Retallack 2008, 2011, 2012, 2013*a*). There are also close associations of red colour with these other indications of soil formation, alternation of red and green beds in core (Fig. 4c) and outcrop (Fig. 4a, b, d and e), and red clasts in green matrix (Fig. 6), as evidence that oxidation was syndepositional (Mawson & Segnit 1949). Illite crystallinity studies of Ediacaran claystones confirm that they qualify as lower greenschist metamorphic facies and lack kaolinite or other clays of modern weathering profiles (Retallack 2008, 2012, 2013*a*). Palaeosols of Ediacaran age show a pattern of red coloration comparable with palaeosols of Phanerozoic age (Retallack 1997).

Another diagnostic geochemical signature of palaeosols is negative strain (volume loss) and negative mass transfer (leaching) of weatherable elements (Brimhall *et al.* 1992). Negative strain was calculated from titania, which is in weather-resistant minerals such as ilmenite, concentrated in the upper part of the profile during weathering. All the named palaeosols show this effect, which is especially well demonstrated by the Vidla palaeosol (Fig. 8). Unweathered sedimentary beds (Ulupa siltstone and shale of Fig. 8), on the other hand, have heavy minerals such as ilmenite at the bottom of the bed, and so show little or positive strain. Loss of silica, alumina and bases (Ca, Mg, Na, K) in the named palaeosols (Fig. 8) is consistent with hydrolytic weathering on land, rather than marine diagenesis (Retallack 1997).

Further evidence for palaeosols is observation that Acraman impact ejecta in Bunyeroo Gorge (Fig. 6) and elsewhere (Wallace *et al.* 1990; Hill *et al.* 2007) was ungraded, and so could not have fallen through water, but instead was deposited on land. Its variation in thickness is comparable with megaripples of base-surge deposits (Crowe & Fisher 1973). Overlying sandstones attributed to tsunami (by Wallace *et al.* 1990; Williams & Gostin 2005) also are indications of shallow marine to terrestrial palaeoenvironments, and not deep shelf facies, for the Bunyeroo Formation (Haines 1988; Calver 2000). The Vulda palaeosol below the impact ejecta layer is unusual in showing a thick drab-coloured top, perhaps owing to burial diagenesis of entrained organic matter, commonly seen in palaeosols (Retallack 1997).

Palaeokarst

Also yielding unusually negative values of $\delta^{13}C$ in Cambrian and Ediacaran rocks of South Australia were reddened (Fig. 4e) or massive carbonate (Fig. 4f), unlike associated grey fossiliferous marine limestones (Retallack 2008, 2011, 2012, 2013*a*). These palaeokarst and palaeocanyon carbonates are very different in $\delta^{13}C$ and $\delta^{18}O$ composition from associated marine limestones (Fig. 7a). Reddened and micritized palaeokarst carbonate also needs to be distinguished from marine carbonate in identifying marine isotopic anomalies (Fig. 2).

Ferruginization, micritization and correlative $\delta^{13}C$ and $\delta^{18}O$ in the Vidla palaeosol atop and within boulders of limestone deep within the palaeocanyon fill (Figs 4f, g and 5c, d) supports the view of Eickhoff *et al.* (1988), von der Borch *et al.* (1989) and Christie-Blick *et al.* (1990) that the canyons were subaerial, with later marine fill (Fig. 9). The Vidla palaeosol was called the 'veneer' by Eickhoff *et al.* (1988) and 'wall plaster' by Dyson (2003). No palaeosols were found in Ulupa Siltstone below the palaeocanyon, at a level that would have corresponded to bedrock, rather than saprock or saprolite (Retallack & Roering 2012). Another new finding is coincidence in time of the Wonoka palaeocanyons with the Fauquier Glaciation of Virginia (Hebert *et al.* 2010), supporting a glacioeustatic as well as local salt-tectonic explanation for incision (Dyson 2003; Backé *et al.* 2010; Kernen *et al.* 2012). Such dramatic base-level change was the

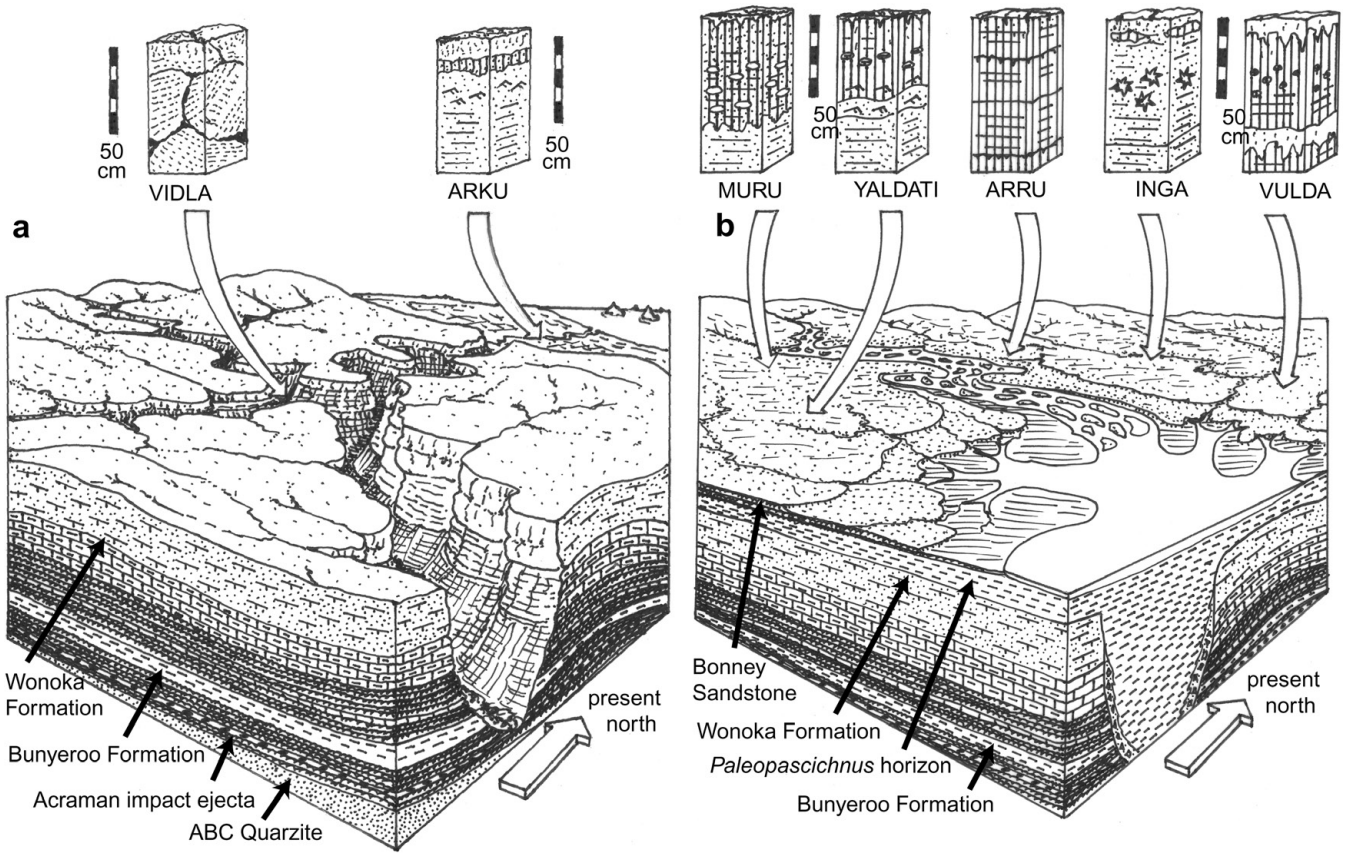

Fig. 9. Conjectural reconstruction of palaeosols and sedimentary palaeoenvironment during deposition in palaeocanyons of the lower Wonoka Formation (**a**) and on floodplains of the lowest Bonney Sandstone (**b**).

main theoretical difficulty for supporters of an entirely submarine origin. The chief argument for entirely submarine canyons made by Giddings *et al.* (2010) is the similarity of carbonate isotopic composition between canyon walls and canyon fill confirmed by Husson *et al.* (2012), but the correlation between $\delta^{13}C$ and $\delta^{18}O$ in Vidla palaeosols is evidence against marine origin (Fig. 7a).

Also persuasive for fluvial incision is the remarkable sinuosity (thalweg trace:distance value of 2.56) of the Fortress Hill palaeocanyon (Fig. 3a and b). Davies & Gibling (2010) argued that meandering streams are unknown before the Silurian origin of land plants. However, meandering channels are known from the Archaean (Button & Tyler 1981), Palaeoproterozoic (Bengtson *et al.* 2007), Neoproterozoic (Dehler *et al.* 2012), and Cambrian (Hereford 1977; Cloyd *et al.* 1990), and remain common on low-relief, unvegetated, muddy, tidal flats today (Kleinhans *et al.* 2009). Modern submarine canyons, in contrast, are generally straight (Green & Uken 2008; Kane *et al.* 2010), with meandering reaches only within the zone of Quaternary sea-level fall (Stevens *et al.* 2014). The marine nature of palaeocanyon fills is supported by grey calcarenites with hummocky stratification and oscillation ripples indicative of very shallow water (Eickhoff *et al.* 1988; Christie-Blick *et al.* 1990; Giddings *et al.* 2010), like shallow shelf facies of the Wonoka Formation elsewhere (Haines 1988).

Alternatives to glacial drawdown of sea level to explain the Wonoka palaeocanyons include uplift by local diapirs aided by salt tectonics (Dyson 2003; Backé *et al.* 2010; Kernen *et al.* 2012), Messinian-style sea-level drop in a restricted evaporitic basin (Christie-Blick *et al.* 1990), and mantle-plume uplift (Williams & Gostin 2000). Evidence against these views comes from recognition of palaeocanyons 600 m deep in the Officer Basin (Sukanta *et al.* 1991) and 700 m deep near Oodnapanicken and Mount Goddard (Fig. 1; Husson *et al.* 2012), thus indicating consistent relative sea-level fall over the entire 1000 km diameter of the Gawler Craton (Williams & Gostin 2000). The Wonoka Formation does include isolated gypsum crystals (Calver 2000), but no salt accumulations or megabreccias of Messinian-scale to induce salt tectonics. Salt is now lacking from diapir megabreccias, which were active during the Ediacaran and Cambrian, remobilizing salt from the Early Neoproterozoic (800–830 Ma) Arkaroola and Curdimurka Subgroups (Dyson 2003; Backé *et al.* 2010; Kernen *et al.* 2012). Local uparching around salt-withdrawal minibasins may explain exceptionally deep palaeocanyons, such as the 1500 m deep Fortress Hill–Umberatana palaeocanyons (Fig. 3), which would be an unusually large glacioeustatic fall (Williams & Gostin 2000). Antrim flood basalts considered mantle plume eruptive rocks by Williams & Gostin (2000) are now known to straddle the Early–Middle Cambrian boundary (508 ± 2 to 505 ± 2 Ma: Glass & Phillips 2006), and so were some 60 Ma younger than the Wonoka palaeocanyons.

Palaeoenvironments inferred from palaeosols

Additional information on Ediacaran palaeoenvironments comes from palaeosols of the Bunyeroo Formation to Bonney Sandstone of eight repeated types (Table 1), here given non-genetic pedotype names from the Adnamatna aboriginal language (McEntee & McKenzie 1992). These include Arku (red ochre), Arru (grey), Inga (hard rock outcrop), Muru (whitish stone), Vidla (rind, crust, dry stuff), Vulda (muscle, flesh), Wadni (thin), and Yaldati (red).

Table 2. *Pedotype interpretation of the Bonney, Wonoka and Bunyeroo Formations*

Pedotype	Climate	Organisms	Topographic setting	Parent material	Time for formation (years)
Vulda	Cool temperate (MAT 8.9 ± 0.4 °C), arid (MAP 377 ± 149 mm) and non-seasonal (MARP 32 ± 22 mm)	Supratidal microbial earth including discoids and small fronds	Supratidal flats and deflation plains	Quartzo-feldspathic silts	1600–5000
Arku	Not diagnostic of climate	Endolithic microbial crust	Coastal dunes and levees	Calcarenite	100–500
Arru	Not diagnostic of climate	Early successional microbial mats	Coastal stream levees	Quartzose sands	100–500
Inga	Cool temperate (MAT 10.9 ± 0.4 °C), arid (MAP 140 ± 129 mm)	Saline microbial earth, including discoids and *Arumberia*	Saline depressions in alluvial floodplain	Quartzose sand	29000–50000
Muru	Cool temperate (MAT 9.2 ± 0.4 °C), arid (MAP 193 ± 16 mm)	Floodplain microbial earth	Well-drained floodplain	Quartzose sand	29000–45000
Vidla	Not diagnostic of climate	Endolithic microbial crust	Crusts on valley-bottom talus boulders	Calcarenitic limestone breccia	100–500
Wadni	Not diagnostic of climate	Early successional microbial mats	Streamside levees	Quartzo-feldspathic silt	100–500
Yaldati	Cool temperate (MAT 10.4 ± 0.4 °C), arid (MAP 407 ± 149 mm) and non-seasonal (MARP 39 ± 22 mm)	Floodplain microbial earth	Well-drained aeolian–alluvial floodplain	Quartzo-feldspathic silt	5000–22000

MAT, mean annual temperature; MAP, mean annual precipitation; MARP, mean annual range of precipitation.

Inga, Muru, Wadni and Yaldati pedotypes have been described previously for the Rawnsley Quartzite (Retallack 2012, 2013*a*).

The various pedotypes of palaeosols can be identified within modern soil classifications (Table 1), such as those of the USA (Soil Survey Staff 2010), the Food and Agriculture Organization (1975, 1978), and the Australian classification (Isbell 1996). The most similar North American soilscapes to shallow-calcic Vulda and Yaldati sequences of the upper Bunyeroo and Wonoka Formations and Bonney Sandstone are Xerosols with subordinate Solonchaks (map X16-1a of Food and Agriculture Organization 1975) in the floodplain of the upper Rio Grande River east of Alamosa, Colorado, where vegetation is western sagebrush (*Artemisia tridentata*) steppe. In Asia, similar soilscapes are Xerosols of the Emba River floodplain (map units Xl 16-1ab and Jc 53-2c of Food and Agriculture Organization 1978) near Atyrau, Kazakhstan, where vegetation is Turan desert semishrub with distinct patches of calcicoles such as sagebrush (*Artemisia terrae-albae*) and halophytes such as saltwort (*Salsola arbuscula*). Alamosa has a mean annual temperature of 4.8 °C and mean annual precipitation of 184 mm (US climate data, 2013, from www.usclimatedata.com), and for Gurjev near Atyrau these values are 7.8 °C and 164 mm (Müller 1982). Similar palaeoenvironments are also indicated by particular palaeosol features outlined below and in Table 2.

Palaeotopography

Two areas of palaeocanyons have been found in the Flinders Ranges: a northern area of palaeocanyons 600–1500 m deep draining northward, and a southern region of palaeocanyons draining southward (Figs 1 and 3). The palaeocanyons cut across the grain of local folding, including such weather-resistant units as the Nuccaleena Formation, and were thus antecedent streams (von der Borch *et al.* 1985). Synsedimentary deformation into local domes was produced by salt diapirs (Dyson 2003; Backé *et al.* 2010; Kernen *et al.* 2012), and this may account for apparent depths of 1500 m of some canyons (von der Borch *et al.* 1985). More generally the canyons are 600–700 m deep (Fig. 9a: Sukanta *et al.* 1991; Husson *et al.* 2012).

During fill of the canyons they would have been drowned valleys, like Sydney Harbour (Scheffers & Scheffers 2012), but palaeocanyons were covered by grey shales of the upper Wonoka Formation. During deposition of the Patsy Hill Member of the lower Bonney Sandstone much of the central Flinders Ranges was an alluvial coastal plain, passing eastward into intertidal flats (Haines 1988; Reid & Preiss 1999). These coastal plains were largely above water table, as indicated by red Vulda and Arru palaeosols with low FeO/Fe_2O_3 ratios. The array of different palaeosols and their associated facies is evidence for a variety of supratidal flats (Arru, Vulda), coastal terraces (Yaldati), levees (Inga) and salinas (Muru) on these coastal plains (Haines 1988; Kernen *et al.* 2012).

Former parent material

Parent materials to palaeosols of the middle and upper Wonoka Formation, including megabreccia palaeocanyon fills, were largely limestone, which was either micritized with little oxidation (Vidla; Fig. 4f) or strongly oxidized and partly brecciated (Arku; Fig. 4e). Thick and regionally extensive brecciated palaeokarst palaeosols are also well known at other stratigraphic levels in the Flinders Ranges (Fig. 2), within the Cryogenian Trezona Formation (McKirdy *et al.* 2001), and the Early Cambrian Wilkawillina Limestone (Clarke 1990).

Palaeosols of the Bunyeroo and lower Wonoka Formations and of the Bonney Sandstone were largely quartzofeldspathic. The upper Bonney Sandstone is quartz rich, but high abundance of feldspar in the Bunyeroo Formation and lower Bonney Sandstone is a general feature of early Palaeozoic and Ediacaran alluvial sandstones and palaeosols (Retallack 2008, 2012).

Time for formation

Estimates of time for formation of single palaeosols come from the diameter of carbonate nodules. In desert soils of New Mexico (Retallack 2005) diameter of carbonate nodules (S in cm) is related to soil age (A in ka) by the equation

$$A = 3.92S^{0.34} \quad (4)$$

($R^2 = 0.57$; SE ±1.8 ka).

Vulda palaeosols of the Bunyeroo and Wonoka Formations and lower Bonney Sandstone have small nodules (3–10 mm; average of 93 examples is 5.0 ± 3.2 mm), corresponding to formation times of

3.3 ± 1.8 ka (range 1.6–5.5 ka). In contrast, Yaldati palaeosols have large nodules (10–40 mm; average of 17 is 15.8 ± 9.6 mm) corresponding to formation times of 8.3 ± 1.8 ka (range 5.5–22.0 ka). Muru and Inga palaeosols are comparable with those of the Ediacara Member, for which durations of (29.7–45.6) ± 15 ka have been proposed (Retallack 2013*a*). Wadni, Vidla, Arku and Arru palaeosols are weakly developed, with common relict sedimentary structures, and so represent much less time for formation, perhaps only a few centuries (Retallack 1997).

Palaeoclimate

Most pedogenic palaeothermometers (Sheldon *et al.* 2002; Gallagher & Sheldon 2013) are based on modern forest to desert shrubland soils, and a better choice for Ediacaran palaeosols predating the evolution of modern vegetation is the pedogenic palaeothermometer of Óskarsson *et al.* (2009), based on modern soils under tundra vegetation of Iceland. This linear regression between mean annual temperature (T in °C) and chemical index of weathering ($I = 100mAl_2O_3/(mAl_2O_3 + mCaO + mNa_2O)$, in molar proportions, is given as

$$T = 0.21I - 8.93 \quad (5)$$

($R^2 = 0.81$; SE ±0.4 °C).

These calculations give temperate mean annual palaeotemperatures for the Bonney Sandstone: in stratigraphic succession, 8.9 ± 0.4 °C for the Vulda sandy clay loam, 10.9 ± 0.4 °C for the Inga sandy clay loam, 10.4 ± 0.4 °C for the Yaldati sandy loam and 9.2 ± 0.4 °C for the Muru sandy loam. Other palaeothermometers gave temperate results as well: *c*. 5 °C cooler (±4.4 °C) for alkali index (Sheldon *et al.* 2002) and *c*. 5 °C warmer (±2.1 °C) for palaeosol weathering index (Gallagher & Sheldon 2013).

Arid palaeoclimate for the palaeosols of the Bunyeroo and Wonoka Formation and Bonney Sandstone are indicated by free carbonate and gypsum sand crystals in the palaeosols. Depth (D_y in cm) to gypsic (By) horizon in modern soils (Retallack & Huang 2010) follows the equation

$$P = 87.593e^{0.0209D_y} \quad (6)$$

with mean annual precipitation (P in mm; $R^2 = 0.63$, SE ±129 mm). Mean annual precipitation (P in mm) is also related to depth to carbonate nodules (D_k in cm) according to the equation

$$P = 137.24 + 6.45D_k - 0.013D_k^2 \quad (7)$$

($R^2 = 0.52$; SE = ±147 mm). Both training sets are mainly sparsely vegetated soils, including polar soils with no vegetation visible to the naked eye (Retallack 2005; Retallack & Huang 2010).

The spread of nodules within soils, or distance between lowest and highest nodule in the profile (H_o in cm), increases with mean annual range of precipitation, which is the difference in monthly mean precipitation between the wettest and driest month (M in mm), and is given by the equation

$$M = 0.79H_o + 13.71 \quad (8)$$

($R^2 = 0.58$; SE ±22 mm: Retallack 2005).

All three proxies require decompaction of the palaeosols, and in this case the standard (equation (9) after Sheldon & Retallack 2001) for Aridisols was used, giving depth to salts in the original soil (D_s) from depth in the current palaeosol (D_p) for a particular depth of burial (K in km: from Retallack 2013*a*):

$$D_s = \frac{D_p}{-0.62/[(0.38/e^{0.17K}) - 1]}. \quad (9)$$

For the Bunyeroo and Wonoka Formations 72 Vulda palaeosols give 377 ± 62 mm mean annual precipitation and 32 ± 7 mm mean annual range of precipitation, but three Yaldati palaeosols give 394 ± 18 mm mean annual precipitation and 23 ± 2 mm mean annual range of precipitation. Results for the Bonney Sandstone were similar: 36 Vulda palaeosols give 383 ± 40 mm mean annual precipitation and 36 ± 6 mm mean annual range of precipitation, but 12 Yaldati palaeosols give 407 ± 44 mm mean annual precipitation and 39 ± 8 mm mean annual range of precipitation. Also in the Bonney Sandstone are 15 Inga palaeosols giving 140 ± 30 mm mean annual precipitation, and four Muru palaeosols yielding 193 ± 16 mm from equation (6) for depth to gypsum. These are all arid and non-monsoonal.

Such dry palaeoclimates are not unusual for palaeolatitudes of 15° ± 3.6° (Schmidt & Williams 1996), but such low-latitude cool climates are found at higher altitude than 3000 m in the modern tropics and were higher than 2000 m during the last Pleistocene glacial maximum (Porter 2001). Further evidence of Ediacaran low-latitude palaeoclimates cooler than modern ones comes from dropstones as evidence of icebergs in both the Bunyeroo and Billy Springs Formation (Gostin *et al.* 2010; Jenkins 2011). Palaeotemperatures from Ediacaran halite fluid inclusion homogenization of 23 ± 5 °C are also cool for modern tropical oceans, but two outliers (among 58 samples) of up to 39 ± 1 °C may indicate transient heating events (Meng *et al.* 2011).

Ancient life on land

Phosphorus is depleted in moderately developed, but not in weakly developed Ediacaran palaeosols (Fig. 8). Experimental studies of modern soils have shown that only organic ligands can weather phosphorus to this extent from apatite in soils (Neaman *et al.* 2005).

Microtubular disruption of lamination in palaeosols of the Bunyeroo Formation to Bonney Sandstone is sparse in lower parts of the profiles (Fig. 5b), but totally disrupts lamination in the upper part of the profiles (Fig. 5a). These ptygmatically compressed, near-vertical, tubular features, some 10–50 μm in diameter, may have been produced by filamentous microbes, such as cyanobacteria, rhizomorphic fungi, or lichen rhizines of microbial earths (Retallack 2012).

Conclusions

Extreme variation in $\delta^{13}C$ of carbonate from +0.95‰ to −11.33‰, and in $\delta^{18}O$ carbonate from −1.4‰ to −15.7‰ of the global Shuram–Wonoka isotopic anomaly for some 17 Ma (580 m in the age model of equation (3)) has been explained by four separate marine models: (1) extreme euxinic ocean stratification (Calver 2000); (2) unusually large volumes of marine methane (Bjerrum & Canfield 2011); (3) deep meteoritic diagenesis of marine limestone (Swart & Kennedy 2012); (4) deep diagenetic brine mixing (Derry 2010). Evidence against a marine origin of the Shuram–Wonoka excursion is significant correlation of $\delta^{13}C$ and $\delta^{18}O$ of carbonate in both Oman (Grotzinger *et al.* 2011) and South Australia (Fig. 7a), because unaltered marine carbonates show no covariance (Fig. 7e). Carbonate of marine methane seeps is univariant for $\delta^{18}O$ but varied for $\delta^{13}C$, and so forms vertical lines on a $\delta^{13}C$ and $\delta^{18}O$ crossplot (Aiello *et al.* 2001; Peckmann *et al.* 2002). This pattern is identical to 'meteoric sphaerosiderite lines' of wetland palaeosols,

and reflects dominance of $\delta^{18}O$ composition by water composition (Ludvigson *et al.* 1998, 2013). Weak correlation of $\delta^{13}C$ and $\delta^{18}O$ of carbonate is possible with regulated diagenetic fluid mixing (Derry 2010), and with meteoric alteration of limestone, if taken to unusual extremes (Swart & Kennedy 2012). Strong correlation of $\delta^{13}C$ and $\delta^{18}O$ in carbonate is unique to well-drained palaeosols, in which CO_2 is under biologically controlled evaporative and temperature variation (Ufnar *et al.* 2008).

Many of the isotopically light values in the Flinders Ranges came from carbonates of palaeosols and palaeokarsts recognized from sharp tops to gradational ferruginization (Fig. 4b and c) or micritization downward (Fig. 8c and d). Palaeokarsts at the same stratigraphic level as the Shuram–Wonoka excursion in South Australia are closely associated with palaeocanyons, which have been controversial mainly on the point of whether they were excavated as subaerial (Christie-Blick *et al.* 1990) or as submarine canyons (Giddings *et al.* 2010). Both sides in the controversy agree that the upper palaeocanyon fill is marine, because it includes hummocky cross-stratification and stromatolites (von der Borch *et al.* 1989). Trough cross-bedding, oscillation ripples and highly sinuous channels are evidence that the palaeocanyons were subaerially incised (von der Borch *et al.* 1989; Christie-Blick *et al.* 1990). Subaerial incision is also indicated by micritized palaeosols on basal talus breccias with isotopic composition identical to that of clasts and canyon walls (Figs 4f and 8c, d), but not like that of marine fill and cover of the palaeocanyons (Husson *et al.* 2012). Palaeocanyon incision was locally exacerbated by salt tectonics (Dyson 2003; Backé *et al.* 2010; Kernen *et al.* 2012). Glacioeustatic sea-level retreat at the time of the Fauquier Glaciation of Virginia (Hebert *et al.* 2010) is supported by exceptionally low $\delta^{18}O$, and thus cold palaeoclimate, in carbonate palaeosols and clasts at the base of the palaeochannels (Eickhoff *et al.* 1988). The Wonoka isotopic anomaly was thus in part due to an array of palaeosols (isotopically negative small nodules in red shale) and palaeokarst (isotopically negative micritized or ferruginized limestone), which give it an unrealistically long duration.

With palaeokarst and otherwise altered carbonate removed, and taking only the excursion represented by both organic and carbonate carbon in marine rocks, the revised Wonoka isotopic excursion in South Australia was −8‰ for $\delta^{13}C$ organic and −6‰ for $\delta^{13}C$ carbonate and lasted less than a million years (equation (3)). This is comparable with but less than some Permian–Triassic boundary isotopic excursions (Retallack & Krull 2006), such as −15‰ for $\delta^{13}C$ of marine organic matter in Wairoa Gorge, New Zealand (Krull *et al.* 2000), and −6.9‰ for $\delta^{13}C$ for marine carbonate near Siusi, Italy (Newton *et al.* 2004). The Permian–Triassic boundary was a major mass extinction in the history of life, but such overturn cannot be seen from the sparse megafossil record of the Wonoka and Bonney Formations (Haines 2000; Jenkins & Nedin 2007). However, the uppermost Wonoka Formation of the Flinders Ranges and lower Narana Formation of the Officer Basin show a very marked global mass extinction of diverse Ediacaran acritarchs (ECAP assemblage of Grey 2005), and replacement with a low-diversity leiosphere-dominated 'Kotlin–Rovno' or LELP assemblage of Gaucher & Sprechmann (2009). Like the Permian–Triassic life crisis of unusual methane emissions owing to large igneous intrusions (Retallack & Jahren 2008; Retallack 2013*c*), the strictly defined organic–carbonate Wonoka excursion may also have been a greenhouse palaeoclimatic spike. A global warming episode in the uppermost Wonoka Formation would have resulted in marine transgression of the *Palaeopaschicnus* shales (Haines 2000), which terminated valley incision and glacioeustatic drawdown during the Fauquier Glaciation, before renewed chill of the Billy Springs Glaciation (Figs 2 and 9).

K. Lloyd, P. Coulthard, A. Coulthard, K. Anderson and D. Crawford facilitated official permission to undertake research in Flinders Ranges National Park. Fieldwork was funded by the PRF fund of the American Chemical Society, and assisted by C. Metzger and J. Gehling. Discussions with B. Runnegar, J. Gehling, P. Wright, M. Kennedy, S. Xiao, G. Narbonne, D. Erwin and N. Sheldon have been very helpful. B. Logan and M. Willison aided examination and sampling of drillcore at PIRSA, Glenside. J. Palandri helped with carbonate stable isotopic analyses.

References

Aiello, I.W., Garrison, R.E., Moore, E.C., Kastner, M. & Stakes, D.S. 2001. Anatomy and origin of carbonate structures in a Miocene cold-seep field. *Geology*, **29**, 1111–1114.

Backé, G., Baines, G., Giles, D., Preiss, W. & Alesci, A. 2010. Basin geometry and salt diapirs in the Flinders Ranges, South Australia: Insights gained from geologically-constrained modelling of potential field data. *Marine and Petroleum Geology*, **27**, 650–665.

Bengtson, S., Rasmussen, B. & Krapež, B. 2007. The Paleoproterozoic megascopic Stirling biota. *Paleobiology*, **33**, 351–381.

Bjerrum, C.J. & Canfield, D.E. 2011. Towards a quantitative understanding of the late Neoproterozoic carbon cycle. *Proceedings of the National Academy of Sciences of the USA*, **108**, 5543–5547.

Brimhall, G.H., Chadwick, O.A., *et al.* 1992. Deformational mass transport and invasive processes in soil evolution. *Science*, **255**, 695–702.

Burns, S. & Matter, A. 1993. Carbon isotopic record of the latest Proterozoic from Oman. *Eclogae Geologicae Helvetiae*, **86**, 595–607.

Button, A. & Tyler, N. 1981. The character and significance of Precambrian paleoweathering and erosion surfaces in southern Africa. *Economic Geology Anniversary Volume*, **75**, 686–709.

Calver, C. 2000. Isotope stratigraphy of the Ediacaran (Neoproterozoic III) of the Adelaide Rift Complex, Australia, and the overprint of water column stratification. *Precambrian Research*, **100**, 121–150.

Calver, C.R., Crowley, J.L., Wingate, M.T.D., Evans, D.A.D., Raub, T.D. & Schmitz, M.D. 2013. Globally synchronous Marinoan deglaciation indicated by U–Pb geochronology of the Cottons Breccia, Tasmania, Australia. *Geology*, **41**, 1127–1130.

Christie-Blick, N., von der Borch, C.C. & di Bona, P.A. 1990. Working hypothesis for the origin of the Wonoka Canyons (Neoproterozoic), South Australia. *American Journal of Science*, **290A**, 295–332.

Clarke, J.D.A. 1990. An Early Cambrian carbonate platform near Wilkawillina Gorge, South Australia. *Australian Journal of Earth Sciences*, **37**, 471–483.

Cloyd, K.C., Demicco, R.V. & Spencer, R.J. 1990. Cambrian tidal channel system: A new mechanism to produce shallowing-upward sequences. *Journal of Sedimentary Petrology*, **60**, 73–83.

Corkeron, M. 2007. 'Cap carbonates' and Neoproterozoic glacigenic successions from the Kimberley region, north-west Australia. *Sedimentology*, **54**, 871–903.

Corsetti, F.A. & Kaufman, A.J. 2003. Stratigraphic investigations of carbon isotope anomalies and Neoproterozoic ice ages in Death Valley, California. *Geological Society of America Bulletin*, **115**, 916–932.

Crowe, B.M. & Fisher, R.V. 1973. Sedimentary structures in base-surge deposits with special reference to cross-bedding, Ubehebe Craters, Death Valley, California. *Geological Society of America Bulletin*, **84**, 663–682.

Davies, N.S. & Gibling, M.R. 2010. Cambrian to Devonian evolution of alluvial systems: The sedimentological impact of the earliest land plants. *Earth-Science Reviews*, **98**, 171–200.

Dehler, C.M., Porter, S.M. & Timmons, J.M. 2012. The Neoproterozoic Earth System revealed from the Chuar Group of Grand Canyon. *In*: Timmons, J.M. & Karlstrom, K.E. (eds) *Grand Canyon Geology: Two Billion Years of Earth's History*. Geological Society of America, Special Papers, **489**, 49–72.

Derry, L.A. 2010. A burial diagenesis origin for the Ediacaran Shuram–Wonoka carbon isotope anomaly. *Earth and Planetary Science Letters*, **294**, 152–162.

Drexel, J.F., Preiss, W.V. & Parker, A.J. 1993. *The Geology of South Australia. Vol. 1. The Precambrian*. Geological Survey of South Australia Bulletin, **54**.

Dyson, I.A. 2003. A new model for the Wonoka canyons in the Adelaide Geosyncline. *MESA Journal*, **31**, 49–58.

Eickhoff, K.H., von der Borch, C.C. & Grady, A.E. 1988. Proterozoic canyons of the Flinders Ranges (South Australia): Submarine canyons or drowned river valleys? *Sedimentary Geology*, **58**, 217–235.

Fedonkin, M.A., Gehling, J.G., Grey, K., Narbonne, G.M. & Vickers-Rich, P. (eds) 2008. *The Rise of Animals: Evolution and Diversification of the Kingdom Animalia*. Johns Hopkins University Press, Baltimore, MD.

Fike, D., Grotzinger, J., Pratt, L. & Summons, R. 2006. Oxidation of the Ediacaran ocean. *Nature*, **444**, 744–747.

FOOD AND AGRICULTURE ORGANIZATION. 1975. *Soil Map of the World. Volume II: North America*. UNESCO, Paris.

FOOD AND AGRICULTURE ORGANIZATION. 1978. *Soil Map of the World. Volume VIII: North and Central Asia*. UNESCO, Paris.

GALLAGHER, T.M. & SHELDON, N.D. 2013. A new paleothermometer for forest paleosols and its implications for Cenozoic climate. *Geology*, **41**, 647–651.

GAUCHER, C. & SPRECHMANN, P. 2009. Neoproterozoic acritarch evolution. *In*: GAUCHER, C., SIAL, A.N., HALVERSON, G.P. & FRIMMEL, H.E. (eds) *Neoproterozoic–Cambrian Tectonics, Global Change and Evolution: A Focus on Southwestern Gondwana*. Elsevier, Amsterdam, 319–326.

GIDDINGS, J.A., WALLACE, M.W., HAINES, P.W. & MORNANE, K. 2010. Submarine origin for the Neoproterozoic Wonoka canyons, South Australia. *Sedimentary Geology*, **223**, 35–50.

GLASS, L.M. & PHILLIPS, D. 2006. The Kalkarindji continental flood basalt province: A new Cambrian large igneous province in Australia with possible links to faunal extinctions. *Geology*, **34**, 461–464.

GOSTIN, V.A., MCKIRDY, D.M., WEBSTER, L.J. & WILLIAMS, G.E. 2010. Ediacaran ice-rafting and coeval asteroid impact, South Australia: Insights into the terminal Proterozoic environment. *Australian Journal of Earth Sciences*, **57**, 859–869.

GRADSTEIN, F.M., OGG, J.G., SCHMITZ, M.D. & OGG, G.M. 2012. *The Geologic Time Scale 2012*. Elsevier, Amsterdam.

GREEN, A. & UKEN, R. 2008. Submarine landsliding and canyon evolution on the northern KwaZulu–Natal continental shelf, South Africa, SW Indian Ocean. *Marine Geology*, **254**, 152–170.

GREY, K. 2005. *Ediacaran palynology of Australia*. Association of Australasian Palaeontologists Memoir, **31**.

GROTZINGER, J.P., FIKE, D.A. & FISCHER, W.W. 2011. Enigmatic origin of the largest-known carbon isotope excursion in Earth's history. *Nature Geoscience*, **4**, 285–292.

HAINES, P.W. 1987. *Carbonate shelf and basin sedimentation, late Proterozoic, Wonoka Formation, South Australia*. PhD thesis, University of Adelaide.

HAINES, P.W. 1988. Storm-dominated mixed carbonate/siliciclastic shelf sequence displaying cycles of hummocky cross stratification, late Proterozoic Wonoka Formation. South Australia. *Sedimentary Geology*, **58**, 237–254.

HAINES, P.W. 2000. Problematic fossils in the late Neoproterozoic Wonoka Formation, South Australia. *Precambrian Research*, **100**, 97–108.

HALVERSON, G., HOFFMAN, P., MALOOF, A., SCHRAG, D., RICE, A.H.N., BOWRING, S. & DUDAS, F. 2005. Toward a Neoproterozoic composite carbon-isotope record. *Geological Society of America Bulletin*, **117**, 1181–1207.

HEBERT, C.L., KAUFMAN, A.J., PENNISTON-DORLAND, S.C. & MARTIN, A.J. 2010. Radiometric and stratigraphic constraints on terminal Edicaran (post-Gaskiers) glaciation and metazoan evolution. *Precambrian Research*, **182**, 402–414.

HEREFORD, R. 1977. Deposition of the Tapeats Sandstone (Cambrian) in central Arizona. *Geological Society of America Bulletin*, **88**, 199–211.

HILL, A.C., HAINES, P.W., GREY, K. & WILLMAN, S. 2007. New records of Ediacaran Acraman ejecta in drillholes from the Stuart Shelf and Officer Basin, South Australia. *Meteoritics and Planetary Science*, **42**, 1883–1891.

HUANG, C.-M., WANG, C.-S. & TANG, Y. 2005. Stable carbon and oxygen isotopes of pedogenic carbonates in Ustic Vertisols: Implications for paleoenvironmental change. *Pedosphere*, **15**, 539–544.

HUSSON, J.M., MALOOF, A.C. & SCHOENE, B. 2012. A syn-depositional age for Earth's deepest $\delta^{13}C$ excursion required by isotope conglomerate tests. *Terra Nova*, **24**, 318–325.

IRELAND, T.R., FLÖTTMAN, T., FANNING, C.M., GIBSON, G.M. & PREISS, W.V. 1998. Development of the early Paleozoic Pacific margin of Gondwana from detrital-zircon ages across the Delamerian Orogen. *Geology*, **26**, 243–246.

ISBELL, R.F. 1996. *The Australian Soil Classification*. CSIRO Publishing, Collingwood, Vic.

JENKINS, R.J.F. 2011. Billy Springs Glaciation, South Australia. *In*: ARNAUD, E., HALVORSON, G.P. & SHIELDS-ZHOU, G. (eds) *The Geological Record of Neoproterozoic Glaciation*. Geological Society, London, Memoirs, **36**, 693–699.

JENKINS, R.J.F. & NEDIN, C. 2007. The provenance and palaeobiology of a new multi-vaned, chambered frondose organism from the Ediacaran (later Neoproterozoic) of South Australia. *In*: VICKERS-RICH, P. & KOMAROWER, P. (eds) *The Rise and Fall of the Ediacaran Biota*. Geological Society, London, Special Publications, **286**, 195–222.

KANE, I.A., MCCAFFREY, W.D. & PEAKALL, J. 2010. On the origin of paleocurrent complexity within deep marine channel levees. *Journal of Sedimentary Research*, **80**, 54–66.

KASTING, J.F., HOWARD, M.T., WALLMANN, K., VEIZER, J., SHIELDS, G. & JAFFRÉS, J. 2006. Paleoclimates, ocean depth, and the oxygen isotopic composition of seawater. *Earth and Planetary Science Letters*, **352**, 82–93.

KAUFMAN, A.J., JIANG, G., CHRISTIE-BLICK, N., BANERJEE, D.M. & RAI, V. 2006. Stable isotope record of the terminal Neoporoterozoic Krol platform in the lesser Himalaya of northern India. *Precambrian Research*, **147**, 156–185.

KERNEN, R.A., GILES, K.A., ROWAN, M.G. & HEARON, T.E. 2012. Depositional and halokinetic-sequence stratigraphy of the Neoproterozoic Wonoka Formation adjacent to Patawarta allochthonous salt sheet, central Flinders Ranges, South Australia. *In*: ALSOP, G.I., ARCHER, S.G., HARTLEY, A.J., GRANT, N.T. & HODGKINSON, R. (eds) *Salt Tectonics, Sediments and Prospectivity*. Geological Society, London, Special Publications, **363**, 85–105.

KLEINHANS, M.G., SCHUURMAN, F., BAKX, W. & MARKIES, H. 2009. Meandering channel dynamics in highly cohesive sediment on an intertidal mud flat in the Westerschelde estuary, the Netherlands. *Geomorphology*, **105**, 261–276.

KNAUTH, L.P. & KENNEDY, M.J. 2009. The late Precambrian greening of the Earth. *Nature*, **460**, 728–732.

KNAUTH, L.P., BRILLI, M. & KLONOWSKI, S. 2003. Isotope geochemistry of caliche developed on basalt. *Geochimica et Cosmochimica Acta*, **67**, 185–195.

KRULL, E.S., RETALLACK, G.J., CAMPBELL, H.J. & LYON, G.L. 2000. $\delta^{13}C_{org}$ chemostratigraphy of the Permian–Triassic boundary in the Maitai Group, New Zealand: Evidence for high latitude methane release. *New Zealand Journal of Geology and Geophysics*, **43**, 21–32.

LANDING, E. & MCGABHANN, B.A. 2010. First evidence for Cambrian glaciation provided by sections in Avalonian New Brunswick and Ireland: Additional data for Avalon–Gondwana separation by the earliest Palaeozoic. *Palaeogeography, Palaeoclimatology, Palaeoecology*, **285**, 174–185.

LOHMANN, K.G. 1988. Geochemical patterns of meteoric diagenetic systems and their application to studies of paleokarst. *In*: JAMES, N.P. & CHOQUETTE, P.W. (eds) *Paleokarst*. Springer, Berlin, 59–80.

LU, M., ZHU, M., *ET AL*. 2013. The DOUNCE event at the top of the Ediacaran Doushantuo Formation, South China: Broad stratigraphic occurrence and non-diagenetic origin. *Precambrian Research*, **225**, 86–109.

LUDVIGSON, G.A., GONZÁLEZ, L.A., METZGER, R.A., WITZKE, B.J., BRENNER, R.L., MURILLO, A.P. & WHITE, T.S. 1998. Meteoric sphaerosiderite lines and their use for paleohydrology and paleoclimatology. *Geology*, **26**, 1039–1042.

LUDVIGSON, G.A., GONZÁLEZ, L.A., *ET AL*. 2013. Paleoclimatic applications and modern process studies of pedogenic siderite. *In*: DRIESE, S.G. (ed.) *New Frontiers in Paleopedology and Terrestrial Paleoclimatology*. Society of Economic Paleontologists and Mineralogists, Special Papers, **44**, 79–87.

MAWSON, D. 1939*a*. The late Proterozoic sediments of South Australia. *Australian and New Zealand Association for the Advancement of Science Meeting Report*, **24**, 79–88.

MAWSON, D. 1939*b*. The Cambrian sequence in the Wirrealpa Basin. *Transactions of the Royal Society of South Australia*, **63**, 331–347.

MAWSON, D. & SEGNIT, E.R. 1949. Purple slates of the Adelaide System. *Transactions of the Royal Society of South Australia*, **72**, 276–280.

MCENTEE, J. & MCKENZIE, P. 1992. *Ad'ňa-mat'-ňa–English Dictionary*. Nobbs, Burnside, SA.

MCFADDEN, K., HUANG, J., *ET AL*. 2008. Pulsed oxidation and biological evolution in the Ediacaran Doushantuo Formation. *Proceedings of the National Academy of Sciences of the USA*, **105**, 3197–3202.

MCKIRDY, D.M., BURGESS, J.M., *ET AL*. 2001. A chemostratigraphic overview of the late Cryogenian interglacial sequence in the Adelaide Fold–Thrust Belt, South Australia. *Precambrian Research*, **106**, 149–186.

MELIM, L.A., SWART, P.K. & EBERLI, G.P. 2004. Mixing zone diagenesis in the subsurface of Florida and the Bahamas. *Journal of Sedimentary Research*, **76**, 904–913.

MENG, F., NI, P., SCHIFFBAUER, J.D., YUAN, X., ZHOU, C., WANG, Y. & XIA, M. 2011. Ediacaran seawater temperature: Evidence from inclusions of Sinian halite. *Precambrian Research*, **184**, 63–69.

MÜLLER, M. 1982. *Selected Climatic Data for a Global Set of Standard Stations for Vegetation Science*. Junk, the Hague.

NEAMAN, A., CHOROVER, J. & BRANTLEY, S.L. 2005. Implications of the evolution of organic acid moieties for basalt weathering over geological time. *American Journal of Science*, **305**, 147–185.

NEWTON, R.J., PEVITT, E.L., WIGNALL, P.B. & BOTTRELL, S.H. 2004. Large shifts in the isotopic composition of seawater sulphate across the Permian–Triassic boundary in northern Italy. *Earth and Planetary Science Letters*, **218**, 331–345.

ÓSKARSSON, B.V., RIISHUUS, M.S. & ARNALDS, O. 2009. Climate-dependent chemical weathering of volcanic soils in Iceland. *Geoderma*, **189–190**, 635–651.

PECKMANN, J., GOEDERT, J.L., THIEL, V., MICHAELIS, W. & REITNER, J. 2002. A comprehensive approach to the study of methane-seep deposits from the Lincoln Creek Formation, western Washington State, USA. *Sedimentology*, **49**, 855–873.

PORTER, S.C. 2001. Snowline depression in the tropics during the Last Glaciation. *Quaternary Science Reviews*, **20**, 1067–1091.

PORTER, S.M., MEISTERFELD, R. & KNOLL, A.H. 2003. Vase-shaped microfossils from the Neoproterozoic Chuar Group, Grand Canyon: A classification guided by modern testate amoebae. *Journal of Paleontology*, **77**, 409–429.

PREISS, W.V. & FAULKNER, P. 1984. Geology, geophysics and stratigraphic drilling at Depot Creek, southern Flinders Ranges. *Quarterly Geological Notes, Geological Survey of South Australia*, **89**, 10–19.

Reid, P.W. & Preiss, W.V. (eds) 1999. *Parachilna Map Sheet, 1:250,000 Sheet SH54-11*, 2nd edn. South Australian Geological Survey, Geological Atlas Series.

Retallack, G.J. 1997. *A Colour Guide to Palaeosols*. Wiley, Chichester.

Retallack, G.J. 2005. Pedogenic carbonate proxies for amount and seasonality of precipitation in paleosols. *Geology*, **33**, 333–336.

Retallack, G.J. 2008. Cambrian palaeosols and landscapes of South Australia. *Australian Journal of Earth Sciences*, **55**, 1083–1106.

Retallack, G.J. 2011. Neoproterozoic glacial loess and limits to snowball Earth. *Journal of the Geological Society, London*, **168**, 1–19.

Retallack, G.J. 2012. Criteria for distinguishing microbial mats and earths. *In*: Noffke, N. & Chafetz, H. (eds) *Microbial Mats in Siliciclastic Sediments*. Society of Economic Paleontologists and Mineralogists, Special Papers, **101**, 136–152.

Retallack, G.J. 2013*a*. Ediacaran life on land. *Nature*, **493**, 89–92.

Retallack, G.J. 2013*b*. Ediacaran Gaskiers Glaciation of Newfoundland reconsidered. *Journal of the Geological Society, London*, **170**, 19–36.

Retallack, G.J. 2013*c*. Permian and Triassic greenhouse crises. *Gondwana Research*, **24**, 90–103.

Retallack, G.J. & Huang, C.-M. 2010. Depth to gypsic horizon as a proxy for paleoprecipitation in paleosols of sedimentary environments. *Geology*, **38**, 403–406.

Retallack, G.J. & Jahren, A.H. 2008. Methane outbursts from igneous intrusion of coal at the Permian–Triassic boundary. *Journal of Geology*, **116**, 1–20.

Retallack, G.J. & Krull, E.S. 2006. Carbon isotopic evidence for terminal-Permian methane outbursts and their role in extinctions of animals, plants, coral reefs and peat swamps. *In*: Greb, S. & DiMichele, W.A. (eds) *Wetlands Through Time*. Geological Society of America, Special Papers, **399**, 249–268.

Retallack, G.J. & Roering, J.J. 2012. Wave-cut or water-table platforms of rocky coasts and rivers? *GSA Today*, **22**, 4–9.

Retallack, G.J., Wynn, J.G. & Fremd, T.J. 2004. Glacial–interglacial-scale paleoclimatic changes without large ice sheets in the Oligocene of central Oregon. *Geology*, **32**, 297–300.

Scheffers, A.M. & Scheffers, S.R. 2012. Coastlines dominated by ingression of the sea into older terrestrial landforms. *In*: Scheffers, A.M., Scheffers, S.R. & Kelletat, D.H. (eds) *The Coastlines of the World with Google Earth*. Springer, Berlin, 73–96.

Schmidt, P.W. & Williams, G.E. 1996. Palaeomagnetism of the ejecta-bearing Bunyeroo Formation, late Neoproterozoic, Adelaide fold belt, and the age of the Acraman impact. *Earth and Planetary Science Letters*, **144**, 347–357.

Sheldon, N.D. & Retallack, G.J. 2001. Equation for compaction of paleosols due to burial. *Geology*, **29**, 247–250.

Sheldon, N.D., Retallack, G.J. & Tanaka, S. 2002. Geochemical climofunctions from North American soils and application to paleosols across the Eocene–Oligocene boundary in Oregon. *Journal of Geology*, **110**, 687–696.

Soil Survey Staff. 2010. *Keys to Soil Taxonomy*. USDA–Natural Resources Conservation Service, Washington, DC.

Stevens, T., Paull, C.K., Ussler, W., McGann, M., Buylaert, J.-P. & Lundsten, E. 2014. The timing of sediment transport down Monterey Submarine canyon, offshore California. *Geological Society of America Bulletin*, **126**, 103–121, http://dx.doi.org/10.1130/B30931.1.

Sukanta, U., Thomas, B., von der Borch, C.C. & Gatehouse, C.G. 1991. Sequence stratigraphic studies and canyon formation, South Australia. *PESA (Petroleum Exploration Society of Australia) Journal*, **19**, 68–73.

Surge, D.M., Savarese, M., Dodd, J.R. & Lohmann, K.C. 1997. Carbon isotopic evidence for photosynthesis in Early Cambrian oceans. *Geology*, **25**, 503–506.

Swanson-Hysell, N.L., Rose, C.V., Calmet, C.C., Halverson, G.P., Hurtgen, M.T. & Maloof, A.C. 2010. Cryogenian glaciation and the onset of carbon isotope decoupling. *Science*, **328**, 608–611.

Swart, P.K. & Kennedy, M.J. 2012. Does the global stratigraphic reproducibility of $\delta^{13}C$ in Neoproterozoic carbonates require a marine origin? A Pliocene–Pleistocene comparison. *Geology*, **40**, 87–90.

Ufnar, D.F., Gröcke, D.R. & Beddows, P.A. 2008. Assessing pedogenic calcite stable-isotope values: Can positive linear covariant trends be used to quantify palaeo-evaporation rates? *Chemical Geology*, **256**, 46–51.

van Kranendonk, M.J., Gehling, J.G. & Shields, G.A. 2008. Precambrian. *In*: Ogg, J.G., Ogg, G. & Gradstein, F.M. (eds) *The Concise Geologic Time Scale*. Cambridge University Press, Cambridge, 23–36.

Veizer, J., Godderis, Y. & François, L.M. 2000. Evidence for decoupling of atmospheric CO_2 and global climate during the Phanerozoic eon. *Nature*, **408**, 698–701.

von der Borch, C.C., Grady, A.E., Aldam, R., Miller, D., Neumann, R., Rovira, A. & Eickhoff, K. 1985. A large-scale meandering submarine canyon: Outcrop example from the Late Proterozoic Adelaide Geosyncline, South Australia. *Sedimentology*, **32**, 507–518.

von der Borch, C.C., Grady, A.E., Eickhoff, K., DiBona, P. & Christie-Blick, N. 1989. Late Proterozoic Patsy Springs Canyon, Adelaide Geosyncline: Submarine or subaerial? *Sedimentology*, **36**, 777–792.

Wallace, M.W., Gostin, V.A. & Keays, R.R. 1990. Spherules and shard-like clasts from the late Proterozoic Acraman impact ejecta horizon, South Australia. *Meteoritics*, **25**, 161–165, http://dx.doi.org/10.1111/j.1945-5100.1990.tb00991.x.

Walter, M.R., Krylov, I.N. & Preiss, W.V. 1979. Stromatolites from Adelaidean (Late Proterozoic) sequences in central and South Australia. *Alcheringa*, **3**, 287–305, http://dx.doi.org/10.1080/03115517908527799.

Williams, G.E. & Gostin, V. A. 2000. Mantle-plume uplift in the sedimentary record; origin of kilometre-deep canyons within late Proterozoic successions, South Australia. *Journal of the Geological Society, London*, **157**, 759–768.

Williams, G.E. & Gostin, V. A. 2005. Acraman–Bunyeroo impact event (Ediacaran), South Australia, and environmental consequences: Twenty five years on. *Australian Journal of Earth Sciences*, **52**, 607–620.

Williams, G.E., Gostin, V.A., McKirdy, D.M. & Preiss, W.V. 2008. The Elatina glaciation, late Cryogenian (Marinoan Epoch), South Australia: Sedimentary facies and palaeoenvironments. *Precambrian Research*, **163**, 307–331.

Xiao, S., Zhou, C., Liu, P., Wang, D. & Yuan, X. 2013. Phosphatized acanthomorphic acritarchs and related microfossils from the Ediacaran Doushantou Formation at Weng'an (South China) and their implications for biostratigraphic correlation. *Journal of Paleontology*, **88**, 1–67.

Received 31 January 2014; revised typescript accepted 11 April 2014.
Scientific editing by Quentin Crowley.